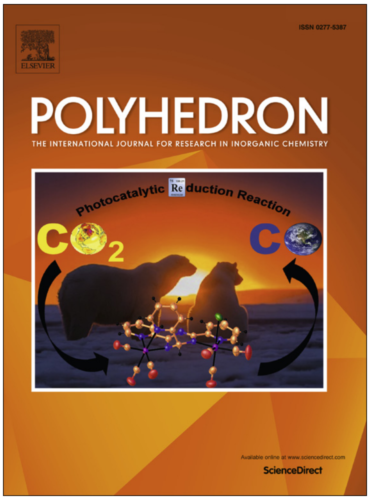

One-dimensional copper(II) coordination polymers built on 4'-substituted 4,2':6',4''- and 3,2':6',3''-terpyridines: Syntheses, structures and catalytic properties

Li Li, Yuan Zhuo Zhang, Chengxiong Yang, E. Liu, James A. Golen, Guoqi Zhang

PII: S0277-5387(15)00792-5
DOI: http://dx.doi.org/10.1016/j.poly.2015.12.042
Reference: POLY 11741

To appear in: *Polyhedron*

Received Date: 26 October 2015
Accepted Date: 18 December 2015

Please cite this article as: L. Li, Y.Z. Zhang, C. Yang, E. Liu, J.A. Golen, G. Zhang, One-dimensional copper(II) coordination polymers built on 4'-substituted 4,2':6',4''- and 3,2':6',3''-terpyridines: Syntheses, structures and catalytic properties, *Polyhedron* (2015), doi: http://dx.doi.org/10.1016/j.poly.2015.12.042

One-dimensional copper(II) coordination polymers built on 4'-substituted 4,2':6',4''- and 3,2':6',3''-terpyridines: Syntheses, structures and catalytic properties

Li Li,[a] Yuan Zhuo Zhang,[b] Chengxiong Yang,[a] E Liu,[a] James A. Golen[c] and Guoqi Zhang[b]*

[a] College of Chemical Engineering and Pharmacy, Jingchu University of Technology, Jingmen 448000, China

[b] Department of Sciences, John Jay College and The Graduate Center, The City University of New York, New York, NY 10019, USA

[c] Department of Chemistry, University of Massachusetts, Dartmouth, North Dartmouth, MA 02747, USA

*Corresponding author. Email address: guzhang@jjay.cuny.edu

Keywords: 3,2':6',3''-terpyridine; Copper(II); Coordination polymer; Crystal structure; Catalysis

ABSTRACT: Divergent ligands containing either 4,2':6',4''- or 3,2':6',3''-terpyridine domains (**1**-**4**) with various 4'-substituents are synthesized. The new ligand **4** was fully characterized by standard spectroscopic and mass spectrometric technique. All ligands were then used to prepare four new copper(II) coordination polymers (**5**-**8**) and good quality single crystals were obtained by the layering method. Single crystal X-ray structural analysis reveals that while the structures of compounds **5** and **6** built on 4,2':6',4''-terpyridine ligands feature similar zigzag chains composed of paddle-wheel $\{Cu_2(\mu\text{-}OAc)_4\}$ units, the use of 3,2':6',3''-terpyridine ligands bearing various 4'-substituents lead to different coordination polymers **7** and **8** in which the ligands adopt remarkably distinct binding modes. The copper(II) coordination polymers were employed to the catalytic aerobic oxidations of alcohols mediated by TEMPO radical (TEMPO = 2,2,6,6-tetramethylpiperidinyl-1-oxyl) and the results revealed that the polymers display slightly different catalytic activity towards the oxidation of benzylic alcohol under heterogeneous conditions, and compound **8** was observed to catalyze the reaction in water with almost quantitative yield when a base additive is present.

1. Introduction

Oligopyridines [1] are one class of frequently utilized molecular building blocks in metal-mediated self-assembly of functional coordination polymers (CPs) or frameworks which have found significant applications in supramolecular chemistry, materials and catalysis science [2-8]. 4,2':6',4''-terpyridine (4,2':6',4''-tpy) is a divergent tris-pyridine ligand that differs from the conventional 2,2':6',2''-terpyridine (2,2':6',2''-tpy) by the positions of N-donors in two side pyridyl rings [9]. Since its first employment in the synthesis of a CP in 1998 [10], 4,2':6',4''-tpy and its derivatives have shown increasing importance in metal-mediated self-assembly owing to their versatile coordination chemistry and tunable materials properties in the recent five years [11-16]. Thanks to the facile synthetic protocol of 4'-substituted 4,2':6',4''-tpy ligands, i.e. the one-pot Kröhnke condensation of various aldehydes and 4-acetylpyridine, a number of metal assemblies of these ligands including discrete supramolecules and infinite CPs have been prepared and structurally characterized [11, 12]. Typically, in all known coordination compounds of 4,2':6',4''-tpy derivatives, the parent 4,2':6',4''-tpy unit behaves as a V-shaped bidentate *N*,*N*-donating ligand (with an internal angle of 120°), remaining the central pyridine non-coordinated. Despite the restricted directionality of the *N*,*N*'-donor set of 4,2':6',4''-tpy backbone in coordination chemistry, variations in metal salts (metals and counter ions), 4'-substitutents on ligand and reaction conditions (solvent, temperature, reaction time and methods of crystallization) were found to largely influence the structures of the resulting metal-organic architectures [11-16]. In contrast, 3,2':6',3''-tpy as an isomer of 4,2':6',4''-tpy was surprisingly only little explored and its coordination versatility is not well established [12, 17-24]. Unlike 4,2':6',4''-tpy, 3,2':6',3''-tpy can adopt different ligand conformations upon rotating about the inter-ring C-C bonds, which would lead to various directionalities between metal-coordinating *N*,*N*'-donors as shown in Scheme 1. Therefore, rich coordination chemistry would be anticipated on this type of ligand, in particular if different 4'-substitutents are introduced.

In continuation with our recent work on zinc(II) or cobalt(II)-driven self-assembly of diverse CPs based on 4,2':6',4''-tpy derivatives [13-16, 24, 25], in this paper we focus on the copper coordination chemistry of four 4'-substituted 4,2':6',4''- or 3,2':6',3''-tpys (**1**-**4**, Scheme 2), of which ligand **4** was unexplored. Because of the significant impact of 4'-substituents on the structures of the resulting coordination assemblies [11-13], variously substituted 4,2':6',4''-tpys (**1** and **2**) and 3,2':6',3''-tpys (**3** and **4**) were chosen, of which ligands **2** and **3** contain the same 4'-substituent, allowing for a direct comparison upon copper(II) complexation. We report the reactions of $Cu(OAc)_2$ with **1-4** and describe the solid-state structures of four new one-dimensional copper(II) CPs resulting from these reactions. Compared to other *d*-block metals, copper was scarcely investigated in the coordination chemistry of 4,2':6',4''-tpy and not even known for 3,2':6',3''-tpy [26, 27]. Built on our previous report on the catalytic applications of Zn-CPs with 4,2':6',4''-tpy derivatives in heterogeneous esterification reactions, herein we also investigate the catalytic ability of new Cu-CPs for TEMPO-mediated aerobic alcohol oxidation, in order to extend the applications of new hybrid materials derived from tpy ligands.

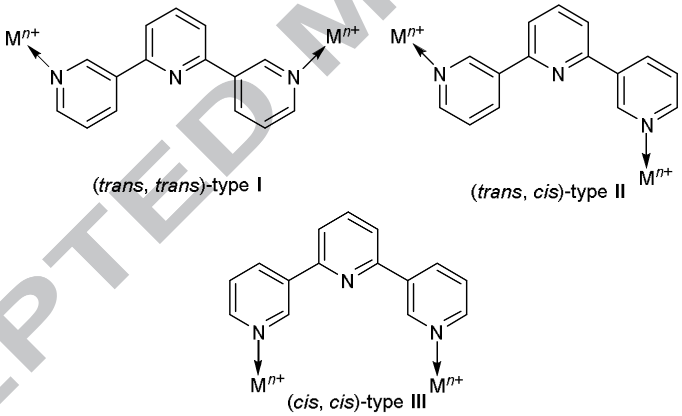

Scheme 1. The schematic representation of three possible metal binding modes of 3,2':6',3''-tpy.

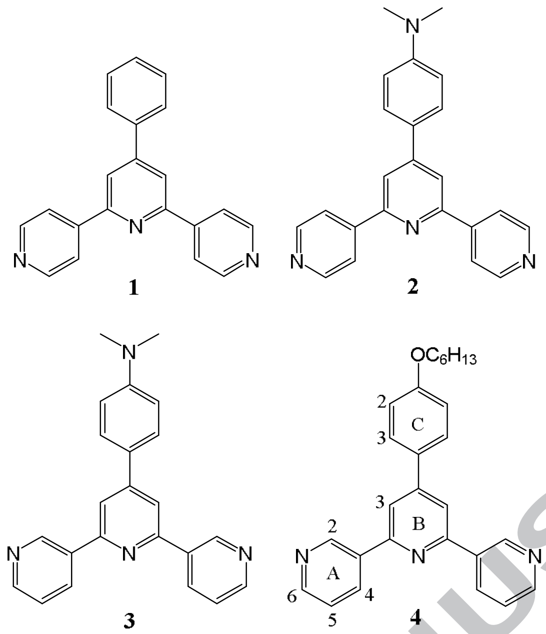

Scheme 2. The structures of 4,2':6',4''- and 3,2':6',3''-tpy ligands **1**-**4** and atomic labelling (**4**) for NMR spectroscopic assignments.

2. Experimental Section

2.1. General

Solvents and reagents were purchased from Fisher Scientific or Sigma-Aldrich in the US. All reactions were performed under ambient conditions. Solution ^{1}H and ^{13}C NMR spectra were obtained at room temperature on a Bruker III 500 MHz spectrometer with TMS as an internal standard. FT-IR spectra were measured on a Shimadzu 8400S instrument with solid samples using a Golden Gate ATR accessory. Elemental analyses were performed by Midwest Microlab LLC in Indianapolis, and GC-MS analysis was carried out on a Shimadzu GCMS-QP2010S gas chromatography mass spectrometer. Ligands **1**-**3** were synthesized according the literature procedure [13-16, 24].

*2.2. Synthesis of 4'-(4-hexyloxyphenyl)-3,2':6',3''-terpyridine (**4**)*

In a 250 cm^3 round-bottom flask equipped with a magnetic stirrer, 3-acetylpyridine (2.42 g, 20.0 mmol) was added to a solution of 4-hexyloxybenzaldehyde (2.06 g, 10.0 mmol) in EtOH (40 cm^3). KOH pellets (0.56 g, 10 mmol) were then added, followed by aqueous NH_3 (28%, 40 cm^3). The resulting orange solution was stirred at room temperature overnight, during which time a white suspension had formed. White solid was collected by filtration, washed with H_2O and EtOH, and dried in vacuo over P_2O_5. Yield: 0.95 g (23%). ^{1}H NMR (500 MHz, $CDCl_3$) δ 9.39 (d, *J* = 2.0 Hz, 2 H, H^{A2}), 8.72 (dd, *J* = 4.5, 1.5 Hz, 2 H, H^{A6}), 8.54 (dt, *J* = 8.0, 2.0 Hz, 2 H, H^{A4}), 7.95 (s, 2 H, H^{B3}), 7.73 (dd, *J* = 7.0, 2.0 Hz, 2 H, H^{C2}), 7.49 (dd, *J* = 13.0, 5.0 Hz, 2 H, H^{A5}), 7.08 (d, *J* = 8.5 Hz, 2 H, H^{C3}), 4.07 (t, *J* = 6.5 Hz, 2 H, H^{OCH2}), 1.86 (m, 2 H, H^{CH2}), 1.52 (m, 2 H, H^{CH2}), 1.39 (m, 4 H, H^{CH2}), 0.95 (t, *J* = 7.0 Hz, 3 H, H^{CH3}) ppm. ^{13}C NMR (125 MHz, $CDCl_3$) δ 160.48, 155.21, 150.45, 149.97, 148.25, 134.89, 134.73, 130.04, 128.33, 123.71, 117.23, 115.26, 68.26, 31.60, 29.19, 25.74, 22.64, 14.09 ppm. FT-IR (solid, cm^{-1}): 1602s, 1516s, 1476m, 1416m, 1397m, 1239s, 1186s, 1119m, 1023s, 832m, 809s, 702s, 657w, 601m. Anal. Calcd. for $C_{27}H_{27}N_3O$: C 79.19, H 6.65, N 10.26%. Found C 78.85, H 6.56, N 9.87%.

2.3. Preparation of $[Cu_2(\mathbf{1})(OAc)_4]_n$ (**5**)

A solution of **1** (30.9 mg, 0.050 mmol) in $MeOH/CH_2Cl_2$ (10 cm^3, 1: 4, v/v) was placed in a test tube. A mixture of MeOH and CH_2Cl_2 (5 cm^3, 1: 1, v/v) was layered on the top of this solution, followed by the solution of $Cu(OAc)_2{\cdot}H_2O$ (19.9 mg, 0.100 mmol) in MeOH (10 cm^3). The tube was sealed and allowed to stand at room temperature for two weeks, during which time X-ray quality green crystals had formed on the wall of the tube. The crystals were collected by decanting the solvent and were washed with MeOH and dried in air. Yield: 41.0 mg (61.1%). FT-IR (solid, cm^{-1}) 1638s, 1617s, 1591s, 1426s, 1223m, 1067m, 1027m, 850s, 825s, 665s, 650m, 619s, 522s. Anal. Calcd. for $C_{29}H_{27}Cu_2N_3O_8$: C 51.78, H 4.05, N 6.25%. Found C 52.01, H 4.12, N 6.21%.

2.4. Preparation of $[Cu_2(\mathbf{2})(OAc)_4]_n$ (**6**)

The same procedure as for **5** was applied to the synthesis of CP **6**, except that ligand **2** was used (35.2 mg, 0.100 mmol). Green block-like crystals were isolated after two weeks. Yield: 49.0 mg (68.6%). FT-IR (solid, cm^{-1}) 1622s, 1591s, 1530s, 1503w, 1428s, 1372m, 1207w, 1173w, 1066m, 1019m, 948w, 841m, 811s, 681s, 624m. Anal. Calcd. for $C_{31}H_{32}Cu_2N_4O_8$: C 52.02, H 4.51, N 7.83%. Found C 52.11, H 4.56, N 7.85%.

2.5. Preparation of $[Cu_2(\mathbf{3})(OAc)_4]_n$ (**7**)

The same procedure as for **5** was applied to the synthesis of CP **7**, except that ligand **3** was used (35.2 mg, 0.100 mmol). Green block-like crystals were isolated after two weeks. Yield: 52.0 mg (72.7%). FT-IR (solid, cm^{-1}) 1619s, 1595s, 1529m, 1484w, 1429s, 1366w, 1251w, 1198w, 1056w, 1029m, 946w, 829m, 809s, 704m, 681s, 660m, 628w. Anal. Calcd. for $C_{31}H_{32}Cu_2N_4O_8$: C 52.02, H 4.51, N 7.83%. Found C 51.76, H 4.40, N 7.60%.

2.6. Preparation of $[Cu_2(\mathbf{4})(OAc)_4]_n$ (**8**)

The same procedure as for **5** was applied to the synthesis of CP **8**, except that ligand **4** was used (40.9 mg, 0.100 mmol). Green block-like crystals were isolated after two weeks. Yield: 55.5 mg (71.8%). FT-IR (solid, cm^{-1}) 2932w, 1621s, 1602s, 1546w, 1516m, 1427s, 1291w, 1239m, 1186m, 1122w, 1028m, 937w, 836m, 812s, 700s, 680s, 643w, 625w. Anal. Calcd. for $C_{35}H_{39}Cu_2N_3O_9$: C 54.40, H 5.09, N 5.44%. Found C 53.93, H 4.98, N 5.36%.

Table 1. Structural refinement data for compounds **5-8**.

Compound	**5**	**6**	**7**	**8**
Formula	$C_{29}H_{27}Cu_2N_3O_8$	$C_{31}H_{32}Cu_2N_4O_8$	$C_{31}H_{32}Cu_2N_4O_8$	$C_{35}H_{39}Cu_2N_3O_9$
Formula Weight	672.62	715.71	715.69	772.77
Crystal system	Monoclinic	Monoclinic	Monoclinic	Triclinic
Space group	*I*2/*a*	*I*2/*a*	*I*2/*a*	*P*-1
a/Å	7.9006(18)	8.035(2)	8.3609(7)	8.3546(6)
b/Å	15.207(3)	14.857(4)	14.2179(12)	14.5546(9)
c/Å	24.943(6)	25.782(8)	26.739(2)	16.3920(12)
α/°	90	90	90	72.836(3)
β/°	91.166(4)	91.109(4)	91.758(2)	77.803(3)
γ/°	90	90	90	74.607(3)
U/Å^3	2996.3(12)	3077.1(16)	3177.1(5)	1816.9(2)
D_c/Mg m^{-3}	1.491	1.545	1.496	1.413
Z	4	4	4	2
μ/mm^{-1}	1.472	1.440	1.394	1.226
T/K	100(2)	90(2)	129(2)	120(2)
Reflections/unique	42802/3804	13641/3533	30368/3041	6670/5445
Parameters	194	209	209	461
$R_1{}^a$, $wR_2{}^b$ [$I > 2\sigma(I)$]	0.0286, 0.0347	0.0352, 0.0380	0.0252, 0.0323	0.0431, 0.0568
$R_1{}^a$, $wR_2{}^b$ (all data)	0.0820, 0.0860	0.1062, 0.1094	0.0639, 0.0675	0.1265, 0.1332
GOF	1.035	1.102	1.021	1.023

$^aR_1 = (F_o - F_c)/F_o$. $^bwR_2 = [w(F_o{}^2 - F_c{}^2)^2/w(F_o)^2]^{1/2}$

Table 2. Selected bond lengths (Å) and angles (°) for compounds **5**-**8**.

5			
Cu1–N1	2.1535(15)	Cu1–O1	1.9724(14)
Cu1–O2^{a}	1.9691(13)	Cu1–O3	1.9757(15)
Cu1–O4^{a}	1.9820(14)	Cu1–Cu1^{a}	2.6344(6)
N1–Cu1–Cu1^{a}	178.60(4)		
6			
Cu1–N1	2.1433(18)	Cu1–O1	1.9772(14)
Cu1–O2^{b}	1.9767(18)	Cu1–O3	1.9771(18)
Cu1–O4^{b}	1.9769(18)	Cu1–Cu1^{b}	2.6285(7)
N1–Cu1–Cu1^{b}	177.07(5)		
7			
Cu1–N1	2.1591(15)	Cu1–O2	1.9688(14)
Cu1–O1^{a}	1.9744(15)	Cu1–O4	1.9588(14)
Cu1–O3^{a}	1.9627(14)	Cu1–Cu1^{a}	2.5979(4)
N1–Cu1–Cu1^{a}	178.21(4)		
8			
Cu1–N1	2.154(3)	Cu1–O1	1.975(3)
Cu1–O3	1.971(3)	Cu1–O2^{c}	1.978(3)
Cu1–O4^{c}	1.973(2)	Cu1–Cu1^{c}	2.6134(8)
Cu2–N3	2.157(3)	Cu2–O6	1.971(3)
Cu1–O8	1.965(3)	Cu2–O7^{c}	1.967(3)
Cu2–O9^{c}	1.965(3)	Cu1–Cu1^{c}	2.6047(8)
N1–Cu1–Cu1^{c}	178.41(8)	N3–Cu1–Cu2^{c}	175.84(8)

Symmetry transformations used to generate equivalent atoms: ^{a} –x+ $^{1}/_{2}$, – y + $^{1}/_{2}$, – z; ^{b} – x + $^{1}/_{2}$, – y + $^{1}/_{2}$, – z + ½; ^{c} –x, – y, – z.

2.7. General Procedure for Catalytic Aerobic Oxidation

Under typical conditions, the catalytic reactions were performed in a small vial equiped with magnetic stirers and open to the air. 1.0 mmol of benzyl alcohol, 0.010 mmol (1 mol% based on ligand) of copper(II) CP, TEMPO (0.050 mmol, 5 mol%) and DMAP (5 mol%) were placed in the vial, to which 5 cm^3 of water was sequentially added. The reaction was allowed to stir at room temperature for 10 hours, after which time the products were extracted with ethyl acetate. The organic layer was diluted with dichloromethane and analysed by GC-MS to give the indicated conversions.

2.8. Crystal Structure Determinations

Suitable crystals of **5-8** were mounted on Cryoloops with Paratone-N oil. Data were collected with a Bruker APEX II CCD or a Bruker D8 Venture X-ray instrument using Mo-Kα radiation. Empirical absorption corrections were applied using the SADABS program [28]. The structures were solved by direct methods and refined based on F^2 by the full matrix least-squares methods using SHELXTL [29]. All non-hydrogen atoms were refined anisotropically by full-matrix least squares on F^2 and all hydrogen atoms were placed in calculated positions with appropriate riding parameters. PLATON program SQUEEZE was used to address diffused solvent that are disorder in the structure of **8** [30]. In **8**, positional disorder (with 63.4/36.6 ratio) associated with carbon atoms C24-C27 in the hexyloxy chain of ligand was treated with C-C distance restraints for C23-C24, C24-C25, C25-C26 and C26-C27 set to 1.54 Å and with equal anisotropic displacement parameters for each pair of those carbons. In addition, anisotropic Uij components of C25/C25A and C27/C27A were refined isotropically. All molecular structures and packing figures were drawn with the program Mercury v. 2.4 [31]. The refinement details are summarized in Table 1 and selected bond parameters are listed in Table 2.

3. Results and Discussion

3.1. Synthesis and characterization

Ligands **1-4** were prepared according to the Kröhnke condensation procedure reported in the literature and the synthesis of new ligand **4** is described here [13-16, 24]. The room-temperature reaction of 4-hexyloxybenzaldehyde with two equiv. of 3-acetylpyridine in the presence of KOH followed by addition of excess aqueous ammonia afforded pure **4** as a white solid after isolation by filtration. **4** is well soluble in halogenated solvents such as CH_2Cl_2 and $CHCl_3$, DMF and DMSO, yet slightly soluble in MeOH, EtOH and MeCN. The elemental analysis data match with that calculated, in agreement with the expected structure.

^{1}H and ^{13}C NMR spectra of **4** were recorded in $CDCl_3$ and are also consistent with the molecular structure of the ligand as illustrated in Scheme 1. Good quality single crystals of **5-8** were obtained in reasonable yields by using a layering technique that allows slow diffusion between solutions of the ligands and $Cu(OAc)_2 \cdot H_2O$ in the CH_2Cl_2-MeOH system, while the solution reactions of the metal-ligand mixture in the same solvent system gave immediately precipitates that prevent from further characterization. The bulk samples of **5-8** are insoluble in water and common organic solvents and they are characterized by FT-IR spectroscopy, elemental analysis and X-ray diffraction analysis.

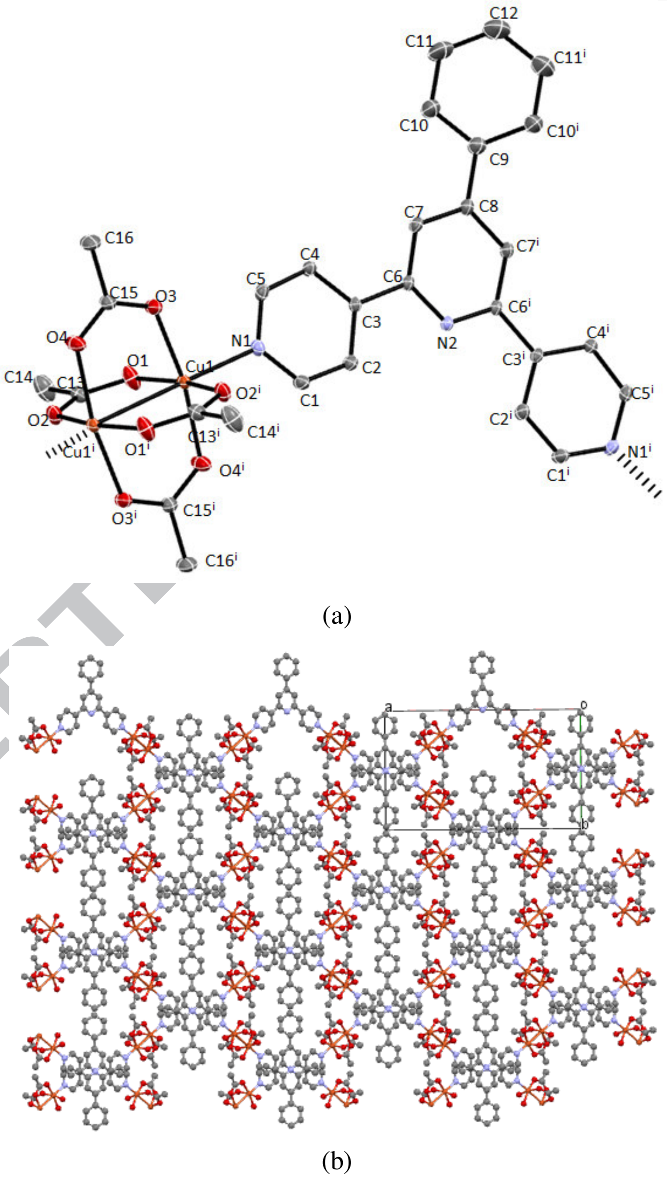

(a)

(b)

Fig. 1. (a) The structure of the repeat unit in **5** with ellipsoids plotted at the 50% probability level, showing the coordination environment around copper(II) centers and bond expansion. (b) The 3D crystal packing model in **5** viewing down the crystallographic *c* axis.

3.2. Crystal Structure of $[Cu_2(\mathbf{1})(OAc)_4]_n$ *(**5**) and* $[Cu_2(\mathbf{2})(OAc)_4]_n$ *(**6**)*

Green blocks of **5** that are suitable for X-ray diffraction analysis were obtained by the layering method described above. **5** crystallizes in the monoclinic space group *I*2/*a* as a one-dimensional coordination polymer with a formula of $[Cu_2(OAc)_4(\mathbf{1})]_n$ (Table 1), which is in agreement with the results of elemental analysis. An ORTEP representation of the repeat unit is depicted in Fig. 1a. The asymmetric unit contains only half of the ligand and the second half was generated by symmetry operation (symmetry code: $-x + {}^1/_2$, $-y + {}^1/_2$, $-z + ½$). In the repeat structural unit, a paddle-wheel $\{Cu_2(\mu\text{-}OAc)_4\}$ motif is observed, which links the ligand **L1** with two of its terminal pyridine-N atoms through its apical positions to form an infinite zigzag chain (Fig. 1b). Similar to the well-known $\{Zn_2(\mu\text{-}OAc)_4\}$ [11], the paddle-wheel $\{Cu_2(\mu\text{-}OAc)_4\}$ unit is common and has been previously found in copper acetate assemblies of 4,2':6',4''-tpys containing various 4'-substituents such as 4'-(biphenyl-4-yl)-4,2':6',4''-tpy and 4'-(pentafluorobiphenyl-4-yl)-4,2':6',4''-tpy [26, 27]. The comparison of cell parameters for crystals of **5** with the known copper CPs, $[Cu_2(\mu\text{-}OAc)_4$(4′-(biphenyl-4-yl)-4,2′:6′,4″-tpy)$]_n$ and $[Cu_2(\mu\text{-}OAc)_4$(4′-(pentafluorobiphenyl-4-yl)-4,2′:6′,4″-tpy)$]_n$ confirms that they are isomorphic. The relevant bond lengths and angles for **5** listed in Table 2 are unexceptional and close to those reported [26, 27]. The Cu…Cu distance of the $\{Cu_2(\mu\text{-}OAc)_4\}$ unit in **5** is 2.6344(6) Å, while that between two copper centers coordinating to the outer-N atoms of one ligand is 12.975(4) Å. The rings of the 4,2':6',4''-tpy domain of ligand are almost planar, and the torsion angle between the outer and central pyridines is only 2.79º, which is in contrast with the large deviation of the 4'-phenyl ring from the plane (torsion angle = 30.02º). The co-planarity of 4,2':6',4''-tpy domains is reflected by the packing mode between the adjacent 1D zigzag chains in **5**. Effective π-stacking interactions of 4,2':6',4''-tpy domains were observed as usually seen in 1D zigzag CPs of Zn(II)- and Cu(II)-4,2':6',4''-tpys. Specifically, both the central pyridine ring and one of the side pyridine rings stack with one another from adjacent polymeric chains with a centroid…centroid distance of 3.655 Å, and the slip angel between two rings for the π-stacking is found to be 64.43°. Unlike the additional inter-chain π…π interactions due to biphenyl…biphenyl stacking found in [Cu_2(μ-OAc)$_4$(4′-(biphenyl-4-yl)-4,2′:6′,4″-tpy)]$_n$, the phenyl groups between chains do not participate in significant π-stacking interactions [26, 27]. The 3-D molecular packing along the crystallographic *c* axis clearly presents the arrangement of chains, showing separate zones of inorganic {Cu_2(μ-OAc)$_4$} units and organic ligands (Fig. 1b).

We next replaced the 4'-phenyl group with 4'-(4-dimethylaminophenyl) group on the 4, 2':6',4''-tpy backbone and tested the reaction of **2** with $Cu(OAc)_2 \cdot H_2O$ by the same layering method as for **5**. As a result, green blocks of [Cu_2(**2**)(OAc)$_4$]$_n$ (**6**) have been harvested and structurally characterized. X-ray structural analysis reveals that **6** is isomorphic to **5** and a similar metal-ligand coordination mode to those found in **5** and other related structures, as illustrated in Fig. 2a. **A**gain 1-D zigzag chains composed of both paddle-wheel {Cu_2(μ-OAc)$_4$} units and C_2-symmetry ligands were observed in the crystal of **6** (Fig. 2b). In **6**, Cu1…Cu1^i separation of 2.6285(7) Å was observed in the {Cu_2(μ-OAc)$_4$} unit and the distance between the adjacent Cu_2 cores is 12.862(3) Å, both close to those found in **5**. Similar to **5**, inter-chain π-stacking of the 4,2':6',4''-tpy domains (the centroid…centroid distance is 3.731 Å, with the slip angle being 61.25°) governs the crystal packing in **6** in the solid state (Fig. 2b).

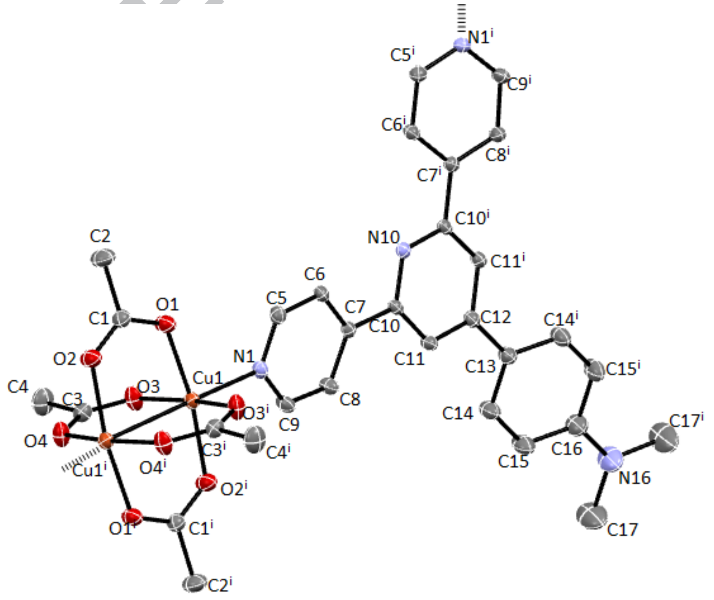

(a)

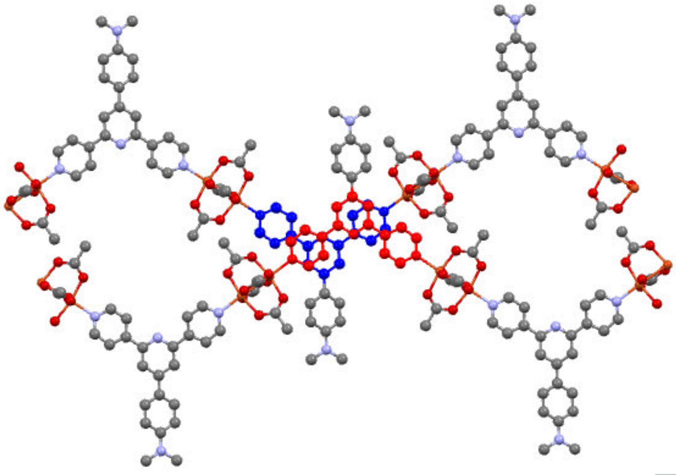

(b)

Fig. 2. (a) The crystal structure of the repeat unit in **6** with ellipsoids plotted at the 50% probability level, showing the coordination environment around copper(II) centers and bond expansion. Hydrogen atoms are omitted for clarity. (b) The packing mode of two adjacent zigzag chains showing inter-chain π-stacking interactions of the tpy domains that are displayed in red and blue, respectively.

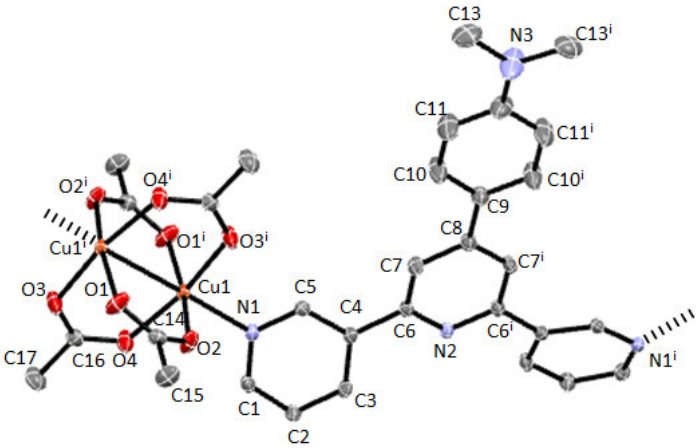

(a)

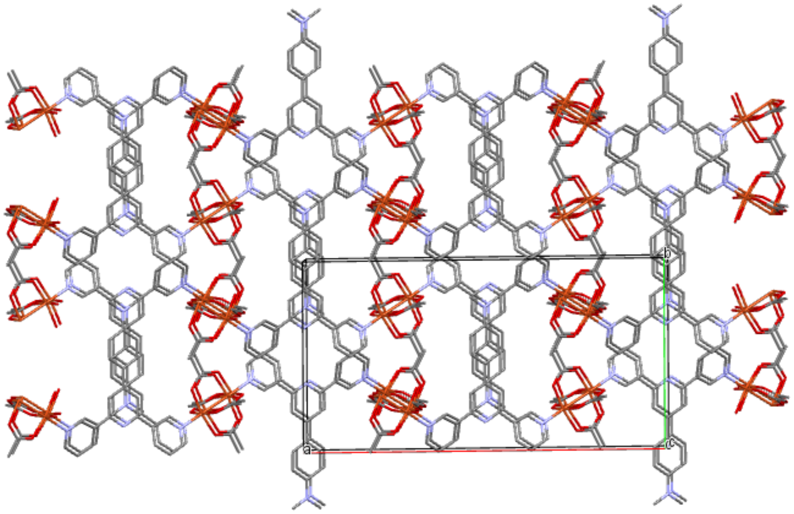

(b)

Fig. 3. (a) The crystal structure of the repeat unit in **7** with ellipsoids plotted at the 50% probability level, showing the coordination environment around copper(II) centers and bond expansion. Hydrogen atoms are omitted for clarity. (b) The 3D crystal packing in **7** along the crystallographic *c* axis.

3.3. Crystal Structure of $[Cu_2(\mathbf{3})(OAc)_4]_n$ *(**7**) and* $[Cu_2(\mathbf{4})(OAc)_4]_n$ *(**8**)*

Since the structures of **5** and **6** are similar to the known copper CPs in the literature, we moved to the related ligand isomers, 3,2':6',3''-tpys. Accordingly, the reaction of **3** with $Cu(OAc)_2 \cdot H_2O$ through the same layering method using MeOH/CH_2Cl_2 solvent system gave good-quality crystals of **7**. Elemental analysis data indicates a metal-ligand ratio of 2:1 in bulk sample of **7**. **7** also crystallizes in the monoclinic space group *I*2/*a* and the cell parameters are similar to those of **5** and **6**, revealing isomorphism in these structures, although the ligands used are essentially different (4,2':6',4''-tpy vs. 3,2':6',3''-tpy). The common paddle-wheel $\{Cu_2(\mu\text{-}OAc)_4\}$ structure is observed again in the repeat unit of the cell and is utilized to bind the outer 3-pyridyl units to form an infinite zigzag chain, in which 3,2':6',3''-tpy moieties adopt a (*trans*, *trans*)-type I binding mode (Scheme 1). The structural similarity observed in CPs **5** and **7** is probably due to the similar V-shaped bidentate binding mode of 3,2':6',3''-tpy (type I) and 4,2':6',4''-tpy (both have internal angles of 120°). In **7**, a slightly shorter $Cu1\ldots Cu1^i$ contact in the $\{Cu_2(\mu\text{-}OAc)_4\}$ core is observed (2.5979(4) Å vs. 2.6344(5) in **5**), while the distance between two Cu centers bonded to the same ligand is a little longer (13.281(2) vs. 12.862(3) Å in **5**). However, what is most distinct between these two structures is the inter-chain molecular packing. Relatively weaker inter-chain π-stacking occurs in the regions of the 4'-(4-dimethylaminophenyl) group and central pyridine of the ligands from adjacent polymeric chains. The centroid…centroid distance between the phenyl rings involved in the π-stacking is 4.430 Å, while the shortest interatomic distance is 3.563 Å. Interestingly, it was observed that in the ligand molecule of **7** the methyl groups are slightly deviated from the of phenyl ring by approximately 4.73º and the torsion angle between phenyl and central pyridyl rings is 6.21º, while the outer 3-pyridyl groups are severely twisted from the central pyridine by a dihedral angle of 20.45º. Furthermore, 1D chains pack in an alternate head-to-tail fashion to form a 3D framework as shown in Fig. 3b. Again, separate organic and inorganic regions are formed upon viewing down the crystallographic *c* axis.

To further examine the influence of 4'-substituents on the copper coordination chemistry with 3,2':6',3''-tpys, we introduced a long alkoxy chain onto the 3,2':6',3''-tpy backbone and prepared the new ligand **4** (Scheme 1). Previously, the 4,2':6',4''-tpy analogue of **4** has been utilized for zinc(II) acetate-mediated self assembly and a discrete complex was formed [25], rather than a coordination polymer. The effect of the chain length of 4'-alkoxylphenyl groups in the 4,2':6',4''-tpy on controlling the resulting Zn^{II} assemblies as coordination polymers or discrete complexes was also systematically investigated [32]. The reaction of **4** with $Cu(OAc)_2·H_2O$ under the same conditions by the layering method afforded green crystals of **8** that are suitable for X-ray structural analysis. **8** crystallizes in the triclinic space group *P*-1 and the repeat structural unit contains one independant ligand molecule and two Cu^{II} centers that constitute similar paddle-wheel $\{Cu_2(\mu\text{-}OAc)_4\}$ units as found in **5**-**7** (Fig. 4a). Note that the presence of a long alkoxy tail in **4** breaks the molecular symmetry of 3,2':6',3''-tpy, and more interestingly, the 3,2':6',3''-tpy motif in **8** coordinates to Cu^{II} centers by the (*trans*, *cis*)-type II binding mode, in sharp contrast to the situation in **7**. This indicates that functionalization on the 4'-position of 3,2':6',3''-tpy did play a crucial role in altering the ligand conformation and hence changing metal coordination modes. In **8**, the Cu…Cu contacts in two independent $\{Cu_2(\mu\text{-}OAc)_4\}$ units are 2.6047(8) and 2.6134(8) Å, respectively, falling in the range of those observed in **5**-**7** (Table 2). However, the distance between Cu1 and Cu2 centers binding to one ligand is significantly shorter (10.932(3) Å) than those in other zigzag chains, due to the *trans*, *cis*-binding mode of **4**. Bond expansion of the repeat structure in Fig. 4 results in the formation of 1D polymeric chain that is clearly different from the zigzag chains described previously. Again, π-stacking interactions between the 1D chains also occur in the domains of the phenyl group and central pyridine of the ligands in a head-to-tail fashion (the shortest interatomic distance for the π…π interaction is 3.574 Å), resulting in the formation of 2D sheets, although the planes of both aromatic rings are twisted with respect to each other with an dihedral angle of 18.45º. Furthermore, π-stacking of the central pyridine domains between 2D sheets leads to a 3D network that is distinct with those of **5**-**7** described above (Fig. 4b).

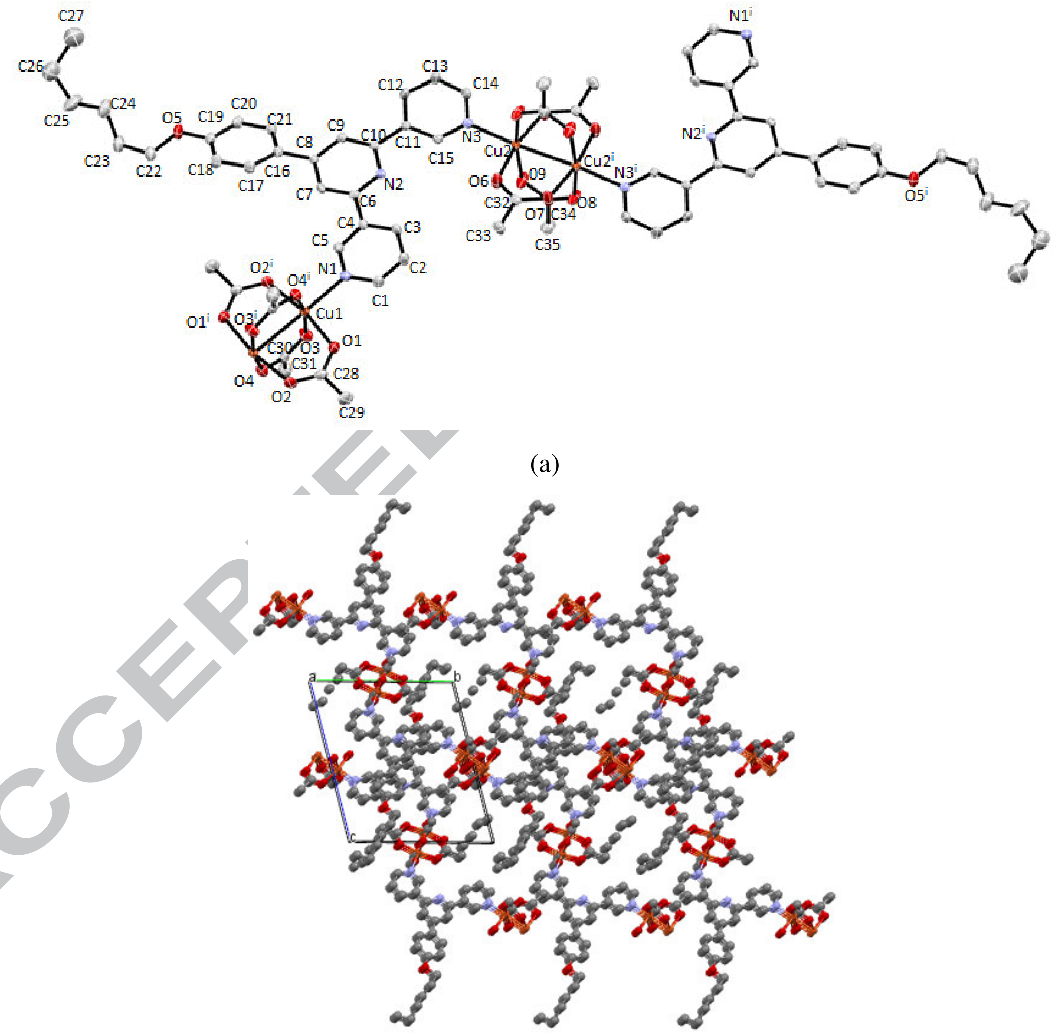

(a)

(b)

Fig. 4. (a) The crystal structure of the repeat unit in **8** with ellipsoids plotted at the 50% probability level, showing the coordination environment around two distinct copper(II) centers. Hydrogen atoms are omitted for clarity. (b) The 3D packing model in crystals of **8** along the crystallographic *c* axis.

3.4. Catalytic Properties

The catalytic aerobic oxidation of alcohols to aldehyde or ketone products is a critical organic transformation that has received considerable attention [33, 34]. Copper-catalyzed TEMPO-mediated aerobic oxidation of alcohols have proven to be the most efficient methodology for this transformation and great attention has been paid to the search of effective combination of copper sources and organic ligands. It has been established that the homogeneous Cu^I/bpy/TEMPO system is the best choice for the oxidation of a large variety of alcohols [34]. Our group has been recently interested in exploring the influence of both different nitrogen ligands and the structures of copper complexes on the catalytic reactivity [35-41] and found that a Cu^{II}/DMAP/TEMPO catalytic system enables aerobic oxidation of a range of alcohols in aqueous media [36, 39]. Despite the significant progress in this field, heterogeneous catalysts involving active Cu-pyridine substructure are little investigated. Due to the poor solubility of CPs **5**-**8** in common solvents and water, we explore the catalytic ability of these organic-inorganic hybrid materials for aerobic alcohol oxidation under heterogeneous conditions, and herein some preliminary results are presented in Table 3. Initially, we tested the reaction of benzyl alcohol in the presence of copper CPs (**5**-**8**, 1 mol%, calculated based on the ligand) and TEMPO (5 mol%) in the air at room temperature when acetonitrile was used as solvent, only poor reactivity (<10% conversion) was observed after 10 h for all the catalysts (entries 1-4). Interestingly, switching the solvent to water improved the performance of all catalysts and the CP **8** was found to be most effective, as 20% conversion of the substrate to benzaldehyde was detected by the GC-MS analysis (entries 5-8). Increasing the catalyst loading of **8** to 5 mol% furnished the reaction with 82% conversion (entry 9). Furthermore, we investigated the effect of a base additive, which has been generally utilized in some effective catalyst systems reported previously. It was found that the addition of DMAP (4-dimethylaminopyridine, 5 mol%) resulted in almost quantitative conversion of benzyl alcohol (entry 10), even though the loading of **8** was low (1 mol%). In contrast, another base additive, triethylamine (TEA) showed a negative influence on the catalytic efficacy (entry 11). It was noted that CP **7** also performed well when DMAP was added under the same conditions. Control experiment using *in situ* combination of free ligand **4** and $Cu(OAc)_2$ in water gave much inferior results (entry 13), indicating the crucial role of metal-organic coordination materials in promoting reactivity. The reaction using ligand 4 without the addition of copper salt gave no reaction, although the combination of $Cu(OAc)_2$ (1 mol%) with DMAP was found to be moderately active (entries 14 and 15) [36]. In addition, TEMPO radical was also required to gain good catalytic activity (entry 16). Substituted benzylic alcohols such as 4-chlorobenzyl alcohol and 4-methoxybenzyl alcohol were also catalytically oxidized to the corresponding aldehydes by using the **8**/DMAP/TEMPO system under heterogeneous conditions, while the secondary alcohol 1-phenylethanol did not proceed well under the optimized conditions (entries 17-19).

Table 3. Copper CPs-catalyzed, TEMPO-mediated aerobic oxidation of benzyl alcohol.[a]

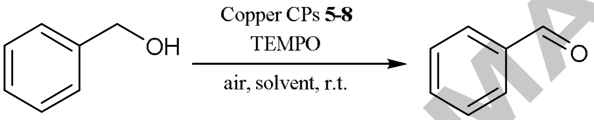

Entry	Copper CP	Additive (5 mol%)	Solvent	Conv.[b] (%)
1	**5**	-	CH_3CN	-
2	**6**	-	CH_3CN	0
3	**7**	-	CH_3CN	9
4	**8**	-	CH_3CN	8
5	**5**	-	H_2O	15
6	**6**	-	H_2O	8
7	**7**	-	H_2O	17
8	**8**	-	H_2O	20
9[c]	**8**	-	H_2O	82
10	**8**	DMAP	H_2O	98
11	**8**	TEA	H_2O	7
12[c]	**7**	DMAP	H_2O	96
13[d]	**4**/$Cu(OAc)_2$	DMAP	H_2O	6
14	**4**	DMAP	H_2O	0

15	$Cu(OAc)_2$	DMAP	H_2O	55
16[e]	**8**	DMAP	H_2O	2
17[f]	**8**	DMAP	H_2O	96
18[g]	**8**	DMAP	H_2O	>99
19[h]	**8**	DMAP	H_2O	5

[a] Condition: 1.0 mmol of the substrate, 1 mol% of copper CP, 5 mol% of TEMPO in solvents (5 mL), 1 atm. air, room temperature, 10 h. [b] Conversions based on GC-MS analysis, aldehyde selectivity > 99% in all cases. [c] 5 mol% of catalyst **8** was used. [d] 2 mol% of copper acetate and 1 mol% of **4** were added sequentially to the reaction system, and a green suspension was developed. [e] Reaction run in the absence of TEMPO. [f] 4-chlorobenzyl alcohol (1.0 mmol) was used. [g] 4-methoxybenzyl alcohol (1.0 mmol) was used. [h] 1-phenylethanol (1.0 mmol) was used.

4. Conclusions

In summary, we present here the syntheses and structural characterization of four copper(II) CPs based on 4,2':6',4''- or 3,2':6',3''-tpy derivatives including the new ligand **4**. In the crystal structures of CPs, a paddle-wheel $\{Cu_2(\mu\text{-}OAc)_4\}$ motif was observed in every case, which linked the bidentate tpy ligands to form 1D polymeric chains with its remaining coordination sites. Although the copper(II) CPs of 4,2':6',4''-tpys feature similar zigzag structures as that reported previously, those derived from 3,2':6',3''-tpys display two different 1D chains, resulting from the differing ligand binding modes of 3,2':6',3''-tpy unit. The effect of 4'-substituents in 3,2':6',3''-tpy is believed to be the determining factor for distinct coordination modes in the present work, although a systematic investigation on the utilization of a broader range of substituents is desired in the future. In addition, these CPs were observed to effectively catalyze the TEMPO-mediated aerobic oxidation of benzylic alcohols under heterogeneous conditions in water.

Acknowledgements

We acknowledge the City University of New York (CUNY) Collaborative Incentive Research Grant (CIRG#80209-06) and the Program for Research Initiatives for Science Majors (PRISM) at John Jay College for support. The Natural Science Foundation of Hubei Province in China (2015CFA130 and 2013CFA015) is gratefully acknowledged.

Appendix A. Supplementary data

CCDC Nos. 1430536-1430539 contain the supplementary crystallographic data for this paper. These data can be obtained free of charge via http://www.ccdc.cam.ac.uk/conts/retrieving.html, or from the Cambridge Crystallographic Data Centre, 12 Union Road, Cambridge CB2 1EZ, UK; fax: (+44) 1223-336-033; or e-mail: deposit@ccdc.cam.ac.uk. Supplementary data associated with this article can be found, in the online version, at http://dx.doi.org/10.1016/j.poly.2015.xx.xxxx.

References

[1] R. P. Thummel, *Comprehensive Coordination Chemistry* II, ed. J. A. McCleverty and T. J. Meyer, Elsevier, Oxford, 2003, vol. 1, p. 41.

[2] A. Wild, A. Winter , F. Schlütter, U.S. Schubert, *Chem. Soc. Rev.* 40 (2011) 1459.

[3] A. Winter, G.R. Newkome, U.S. Schubert, *ChemCatChem* 3 (2011) 1384.

[4] U.S. Schubert, A. Winter, G.R. Newkome, *Terpyridine-Based Materials*, Wiley-VCH, Weinheim, Germany 2011, Ch. 4.

[5] Y. Gao, D. Rajwar, A.C. Grimsdale, *Macromol. Rapid Commun*. 35 (2014) 1727.

[6] A. Winter, M. Gottschaldt, G.R. Newkome, U.S. Schubert, *Curr. Top. Med. Chem.* 12 (2012) 158.

[7] S. Hayami, Y. Komatsu, T. Shimizu, H. Kamihata,Y.H. Lee, *Coord. Chem. Rev.* 255 (2011) 1981.

[8] A. Winter, M.D. Hager, G.R. Newkome, U.S. Schubert, *Adv. Mater.* 23 (2011) 5728.

[9] E.C. Constable, *Chem. Soc. Rev.* 36 (2007) 246-253

[10] M. Barquin, J. Cancela, M.J. Gonzalez Garmendia, J. Quintanilla, U. Amador, *Polyhedron* 17 (1998) 2373.

[11] C.E. Housecroft, *Dalton Trans.* 43 (2014) 6594.

[12] C.E. Housecroft, *CrystEngComm* 17 (2015) 7461.

[13] G. Zhang, Y. Jia, W. Chen, W. F. Lo, N. Brathwaite, J.A. Golen, A.L. Rheingold, *RSC Adv.* 5 (2015) 15870.

[14] Z. Yin, S. Zhang, S. Zheng, J.A. Golen, A.L. Rheingold, *Polyhedron* 101 (2015) 139.

[15] E.C. Constable, G. Zhang, C.E. Housecroft, M. Neuburger and J.A. Zampese, *CrystEngComm* 12 (2010) 3733.

[16] E.C. Constable, G. Zhang, C.E. Housecroft, J.A. Zampese, *CrystEngComm* 13 (2011) 6864.

[17] F. H. Allen, *Acta Crystallogr., Sect. B: Struct. Sci.*, 58 (2002) 380.

[18] B.-C. Wang, X.-L. Chen, H.-M. Hu, H.-L. Yao and G.-L. Xue, *Inorg. Chem. Commun*., 12 (2009) 856.

[19] C. Liu, Y.-B. Ding, X.-H. Shi, D. Zhang, M.-H. Hu, Y.-G. Yin and D. Li, *Cryst. Growth Des.,* 9 (2009) 1275.

[20] J. Granifo, M. Vargas, M. T. Garland, A. Ibanez, R. Gavino, R. Baggio, *Inorg. Chem. Commun.*, 11 (2008) 1388

[21] E. C. Constable, C. E. Housecroft, M. Neuburger, S. Vujovic, J. A. Zampese, G. Zhang, *CrystEngComm* 14 (2012) 3554.

[22] N. Li, Q.-E Zhu, H.-M. Hu, H.-L. Guo, J. Xie, F. Wanga, F.-X. Dong , M.-L. Yang, G.-L. Xue, *Polyhedron* 49, 2013, 207.

[23] Y. M. Klein, E. C. Constable, C. E. Housecroft, A. Prescimone, *CrystEngComm*, 17, 2015, 2070.

[24] E.C. Constable, C.E. Housecroft, M. Neuburger, S. Vujovic, J.A. Zampese, G. Zhang, *CrystEngComm* 14 (2012) 3554.

[25] E.C. Constable, G. Zhang, C.E. Housecroft and J.A. Zampese, *Inorg. Chem. Comm.* 15 (2012) 113**.**

[26] E.C. Constable, C.E. Housecroft, M. Neuburger, J. Schönle, S. Vujovic and J.A. Zampese, *Polyhedron*, 62 (2013) 120.

[27] E.C. Constable, C.E. Housecroft, S. Vujovic, J.A. Zampese, A. Crochet and S.R. Batten, *CrystEngComm* 15 (2013) 10068.

[28] G M. Sheldrick, SADABS, Program for Empirical Absorption Correction of Area Detector Data, University of Göttingen, Germany, 1997.

[29] Sheldrick, G. M. SHELXS-97, Program for the Solution of Crystal Structures, University of Göttingen, Germany, 1997.

[30] A.L. Spek, *Acta Crystallogr., Sect. D: Biol. Crystallogr.* 65 (2009) 148.

[31] Mercury: Visualization and analysis of crystal structures. C.F. Macrae, P.R. Edgington, P. McCabe, E. Pidcock, G.P. Shields, R. Taylor, M. Towler, J. van de Streek, *J. Appl. Crystallogr.* 39 (2006) 453.

[32] Y.M. Klein, E.C. Constable, C.E. Housecroft, J.A. Zampese, A. Crochet, CrystEngComm, 16 (2014) 9915.

[33] B. L. Ryland, S. S. Stahl, *Angew. Chem., Int. Ed.* 53 (2014) 8824 and references therein.

[34] J. M. Hoover, B. L Ryland, S. S. Stahl, *ACS Catal.* 3 (2013) 2599.

[35] G. Zhang, G. Proni, S. Zhao, E.C. Constable, C.E. Housecroft, M. Neuburger, J.A. Zampese, *Dalton Trans.* 43 (2014) 12313.

[36] G. Zhang, C. Yang, E. Liu, L. Li, J.A. Golen, A.L. Rheingold, *RSC Advances* 4 (2014) 61907.

[37] G. Zhang, E. Liu, C. Yang, L. Li, J.A. Golen, A.L. Rheingold, *Eur. J. Inorg. Chem.* (2015) 939.

[38] G. Zhang, L. Li, C. Yang, E. Liu, J.A. Golen, A.L. Rheingold, *Inorg. Chem. Commun.* 51 (2015) 13.

[39] E. Liu, Y.Z. Zhang, L. Li, C. Yang, J.C. Fettinger, G. Zhang, *Polyhedron* 95 (2015) 223.

[40] Z. Yin, G. Zhang, T. Phoenix, S. Zheng, J.C. Fettinger, *RSC Adv.* 5 (2015) 36156.

[41] G**.** Zhang, Y.Z. Zhang, W. Lo, J. Jiang, J.A. Golen, A.L. Rheingold, *Polyhedron* 103 (2016) 227.

Graphic Abstract - Pictogram

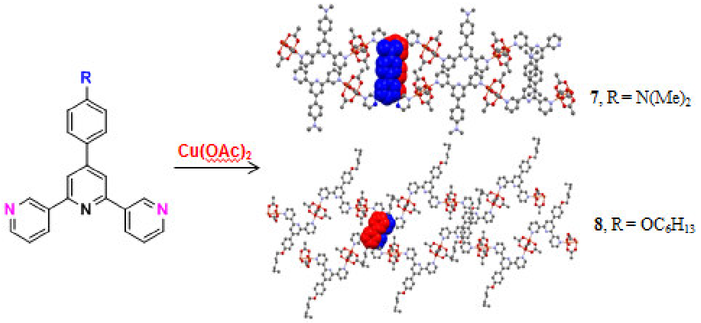

Abstract - Synopsis

Four new Cu(II) coordination polymers based on the divergent ligands containing either 4,2':6',4''- or 3,2':6',3''-terpyridine domains with various 4'-substituents are synthesized and structurally characterized. 4'-Substituents in the 3,2':6',3''-terpyridines are found to affect the ligand binding modes and distinct coordination assemblies are revealed. The catalytic aerobic alcohol oxidation using the crystalline materials was explored under heterogeneous conditions.